3B-Splines in the Integral Equation Solution for Scattering from Bodies of Revolution

F.L. Teixeira[1], J.R. Bergmann[2]
[1]EMBRATEL S.A., Satellite Transmission Department
[2]CETUC - Center for Telecommunication Studies, Catholic University of Rio de Janeiro

Abstract- The use of B-Spline functions is investigated in conjunction with the Method of Moments integral-equation solution to the problem of scattering from conducting bodies of revolution. Its computational performance in terms of relative accuracy and storage/CPU time requirements is evaluated against entire-domain and sampling-like basis functions. Particular attention is given to the description of currents near edges. Questions of time (space) and frequency (wavenumber) localization are also addressed. A simple scheme devised to enforce boundary conditions *a priori* is shown to be potentially capable to stabilize otherwise spurious solutions.

I. INTRODUCTION

The numerical treatment of open-boundary radiation or scattering problems in the frequency domain is usually done with the use of a linear integral equation (IE) formulation. The Method of Moments (MoM) is a general procedure to reduce an IE to a matrix equation [1] that is usually dense and computationally intensive to solve. In order to reduce the matrix dimensions, a crucial aspect of the MoM solution is the adequate choice of basis functions. Two major classes of basis functions commonly employed in the MoM can be identified: entire-domain functions [2-4] and local-domain (compact support) functions [4-6]. Entire-domain functions are more specialized, being used in specific problems to attain a fast convergence. Local-domain functions are geometrically flexible, being more practical to analyze complex geometries.

The fast rate of convergence achieved with the use of entire-domain functions for certain problems of scattering from perfect electric conductors (PECs) [2,3] is related to the spectral characteristic (in the spatial-frequency domain of the wave-number $\bar{k}$) of the induced electric currents. Of particular interest, because of its practical importance, is the class of smooth objects, i.e., with local radius of curvature greater than one wavelength. For these objects, a reasonable assumption is that the induced current has a bandlimited nature, i. e., can be well approximated by functions of confined wavenumber spectrum, $|\bar{k}| < k_m$ (moreover in the context of far-field scattering). Heuristic arguments in favor of this hypothesis were well posed by Hermann [7]. Entire-domain functions as Fourier trigonometric functions usually have a low-frequency spectrum and thus, are natural candidates for an efficient expansion for the unknown currents.

One attractive characteristic of the local-domain functions not shared by the entire-domain functions is local support. It permits a faster evaluation of integrals since only a small region of the scatterer needs to be integrated in the evaluation of each coefficient of the MoM linear system (impedance matrix). In addition, since the entire-domain functions are defined over the whole object, the CPU time for evaluating each coefficient is also dependent on the electric size of the object. As a consequence, it implies an even worse frequency-scaled dependency of the required CPU time to solve the problem.

The interest to develop a scheme combining the attractive aspects of local and entire-domain functions can be traced from the above observations. It would correspond to the use of basis functions having band-limited spectrum and, simultaneously, local support. Ideally speaking, this objective is not strictly possible, since the Fourier transform of any function with a finite spatial support has necessarily an infinite support. The objective to be sought is then an approximation to this ideal.

One scheme that proved successful in this direction was the use of the so-called quasi-localized bandlimited basis functions (sampling-like) [7,8]. In the examples considered there, the sampling rate associated with the MoM was reduced from the usual number of 10 basis functions per wavelength to an average rate of between 2.5 and 3 bandlimited basis functions per wavelength. At the same time these functions allowed a very rapid computation of the integrals involved due to their limited overlap. The basic limitation of this approach is that it does not provide special treatment for currents near the edge of the scatterer (in the case of open scatterers), where a singular behavior is expected in the induced currents (leading to spatially localized high-frequency components). Failure to incorporate the correct edge behavior can result in erroneous currents and anomalous behavior of the solution near the edge [9].

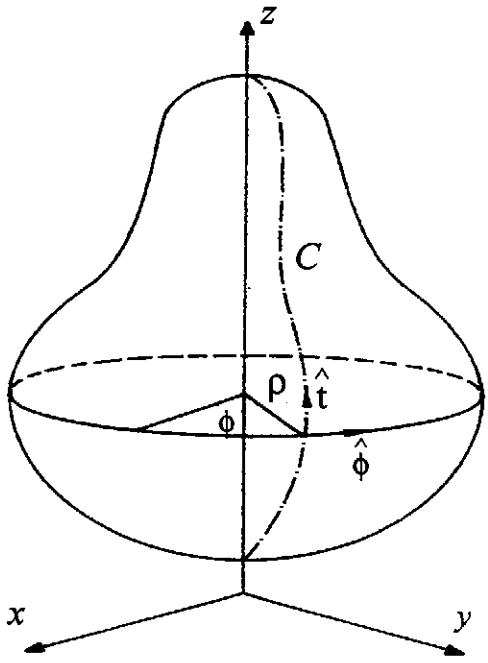

Fig. 1- Geometry and coordinates of a body of revolution

To alleviate these problems, this work explores the use of B-splines in the context of scattering from PEC bodies of revolution (BoR). Among the advantages presented by these functions and herein investigated are: (i) Near-optimal localization on the spatial and spatial-frequency (or wavenumber) domains $(\vec{r},\vec{k})$ with asymptotic convergence to Gaussian functions, which have an optimal localization [10]; (ii) Ability to model the singular behavior near the edges through the use of multiple knots; (iii) Analytical simplicity that permits an exact analytic extraction of singularities arising in the kernel of the IE. Two specific examples are considered: the scattering from an infinitely thin, PEC circular disc, and the scattering from a finite, PEC hollow cylinder. For the second example it is also shown that a simple scheme devised to enforce *a priori* boundary conditions on the longitudinal current component can also solve the problem of instability in the azimuthal component when using the Electric Field Integral Equation (EFIE) [11].

This work is organized as follows. In section II the MoM solution of the electromagnetic scattering from conducting bodies of revolution is briefly reviewed. Section III contains a description of the basis functions used in this paper, with particular attention given to the interesting properties of B-splines. In section IV comparative results from the analysis of a circular disk and a finite hollow cylinder are presented. Finally, section V summarizes the most important conclusions.

II. Method of Moments Solution of the Scattering From Bodies of Revolution

In this section the basic formulation of the MoM analysis of conducting BoRs is briefly reviewed. For a more detailed discussion the reader is referred to [5].

Fig. 1 depicts a general BoR. It is generated by a rotation of the curve C about the z-axis. For numerical purposes, C is approximated by a sequence of linear segments ε_i. Any point on the BoR surface can be described by two coordinates: ϕ, the azimuth angle; and t, the arclength along C. Given an incident electric field $\vec{E}^{inc}$ the solution of the problem follows from the application of the pertinent boundary condition:

$$\hat{n}\times(\vec{E}^{inc}+\vec{E}^{s})=0 \tag{1}$$

on the surface of the PEC scatterer, where $\vec{E}^{S}(\vec{r})$ is the scattered field due to surface currents $\vec{J}(\vec{r}')$ on the body and $\hat{n}$ is the unit normal vector to the surface. The scattered field can be expressed in terms of the induced current through the radiation integral, with an $e^{j\omega t}$ dependency assumed:

$$\vec{E}^{s}(\vec{r})=-j\omega\mu\iint_{s}\vec{J}(\vec{r}')G(\vec{r},\vec{r}')ds'-\frac{j}{\omega\varepsilon}\vec{\nabla}_{s}\iint_{s}(\vec{\nabla}'_{s}.\vec{J})G(\vec{r},\vec{r}')ds' \tag{2}$$

here $G(\vec{r},\vec{r}')$ is the free space Green's function:

$$G(\vec{r},\vec{r}')=\frac{e^{-jk|\vec{r}-\vec{r}'|}}{4\pi|\vec{r}-\vec{r}'|} \tag{3}$$

Combining (1) and (2) the Electric Field Integral Equation (EFIE) is obtained:

$$\vec{E}^{inc}_{\tan}=L(\vec{J})=j\omega\mu\iint_{s}\vec{J}(\vec{r}')G(\vec{r},\vec{r}')ds'+\frac{j}{\omega\varepsilon}\vec{\nabla}_{s}\iint_{s}(\vec{\nabla}'_{s}.\vec{J})G(\vec{r},\vec{r}')ds' \tag{4}$$

By decomposing the induced current and the incident tangential electric field in terms of its (orthogonal) components along the t and ϕ directions, a set of two coupled integro-differential equations is obtained. In a dyadic form they are written as:

$$(L^{tt}\hat{t}\hat{t} + L^{t\phi}\hat{t}\hat{\phi} + L^{\phi t}\hat{\phi}\hat{t} + L^{\phi\phi}\hat{\phi}\hat{\phi})\cdot$$
$$(J_t\hat{t} + J_\phi\hat{\phi}) = E_t^{inc}\hat{t} + E_\phi^{inc}\hat{\phi} \quad (5)$$

where L^{pq} are the integro-differential scalar operators (p and q stand for t and ϕ). The MoM is then applied to solve the above equations. We start by expressing the unknown currents in terms of a suitable set of basis functions:

$$\vec{J}(t,\phi) = \sum_{m=-M}^{N}\left[\sum_{i=1}^{Nt} I_{mi}^{t}\vec{b}_{mi}^{t}(t,\phi) + \sum_{i=1}^{N\phi} I_{mi}^{\phi}\vec{b}_{mi}^{\phi}(t,\phi)\right]$$
$$\vec{b}_{mi}^{t}(t,\phi) = \frac{f_i^t(t)}{\rho(t)}e^{jm\phi}\hat{t}$$
$$\vec{b}_{mi}^{\phi}(t,\phi) = f_i^{\phi}(t)e^{jm\phi}\hat{\phi} \quad (6)$$

The factor $1/\rho(t)$ (radial distance to z-axis) in the t-component serves to cancel the $\rho(t)$ associated with the element of surface $dS' = \rho d\phi dt$. The coefficients in (6) are the unknowns of the problem. The above integro-differential equations in a Hilbert space are transformed (projected) into a matrix equation by inserting (6) in (5) and performing an inner product of the resultant equations with a set of test functions defined as complex conjugates of the basis functions (Galerkin method). The inner product is operationally defined to be the integral over S of the dot product of the basis and test functions. From the choice of harmonic dependence on ϕ, there follows, in view of the rotational symmetry of there problem, a natural decoupling among different modes (index m). The resultant linear system matrix (impedance matrix) exhibits a block diagonal form and each mode can be treated separately, greatly reducing the computational effort to solve the overall problem. The impedance matrix equation for the m-th mode is expressed as:

$$\begin{bmatrix} Z_m^{tt} & Z_m^{t\phi} \\ Z_m^{\phi t} & Z_m^{\phi\phi} \end{bmatrix}\begin{bmatrix} I_m^t \\ I_m^\phi \end{bmatrix} = \begin{bmatrix} V_m^t \\ V_m^\phi \end{bmatrix} \quad (7)$$

$$\left(Z_m^{pq}\right)_{ij} = \left\langle L(\vec{b}_{mj}^{q}), \vec{b}_{mi}^{p^*}\right\rangle$$

$$\left(V_m^p\right)_i = \left\langle \vec{E}^{inc}, \vec{b}_{mi}^{p^*}\right\rangle$$

where $\langle\ ,\ \rangle$ denotes inner product. The right-hand side vector in (7) is called the excitation vector. Explicit expressions for the impedance matrix and excitation vector (plane-wave excitation) elements and can be found in [5]. The solution of the above matrix equation (7) determines the induced electric current according to (6).

The necessary number of modes in a specific problem can be determined from a convergence study. In case of plane-wave axial incidence only the m = ± 1 modes are excited.

III. B-Splines Basis Functions in BOR Analysis

In this section the use of cubic B-splines as the basis functions in t is discussed. The domain of interest is limited to the interval $[0,T_F]$, where T_F is the total arclenght of the generating curve. In order to construct cubic (order n=4, degree n−1=3) B-splines on this bounded interval the first step is to define a partition of K+1 nodal points (knots): $\{\ t_i\ \}_{i=1,K}$, where $0 = t_0 < \ldots < t_K = T_F$. In this work a uniform spaced partition will be used. Additional points are placed at the ends of the interval (multiple knots): $t_{-3} = t_{-2} = t_{-1} = 0$ and $t_{K+1} = t_{K+2} = t_{K+3} = T_F$.

Let's define :

$$\gamma_n(s;t) = (s-t)_+^{n-1} \equiv \begin{cases} (s-t)^{n-1} & s \geq t \\ 0 & s < t \end{cases} \quad (8)$$

Then the (normalized) B-spline of order n is given as the n-th divided difference of $\gamma_n(s;t)$ in s on t_i , ..., t_{i+n} for fixed t [12], i. e.,

$$\beta_{n,i}(t) = (t_{i+n} - t_i)\gamma_n(t_i,\ldots,t_{i+n};t), \text{ for all i} \quad (9)$$

Fig.2 shows cubic B-splines (n = 4) on a unit interval with uniform spacing of five interior knots. Explicit expressions for (9) can be found in [13].

The above cubic B-splines present a series of potential advantages when used as a basis set. First, they have a local support which permits a fast evaluation of the integrals in (7). Second, they are smooth, having a spectrum concentrated at low frequencies, as the Fourier transform of the central B- spline of order n is given by $\beta_n(t) \leftrightarrow \mathrm{sinc}^n(f)$ with $\mathrm{sinc}(f) = \sin\pi f/\pi f$. This is an important characteristic to fast convergence modeling of currents on smooth scatterers, as discussed in section I. B-splines are thus essentially limited both in the spatial (time) and the wavenumber (frequency) domains. Indeed, it can be shown [10] that B-splines converge to Gaussian functions pointwise as the order of the spline

tends to infinite. Gaussian functions are optimal in terms of time/frequency localization. The approximation error for the cubic case is already less than 3% and the variance product is already within 2% of the limit specified by the uncertainty principle (Fig. 3).

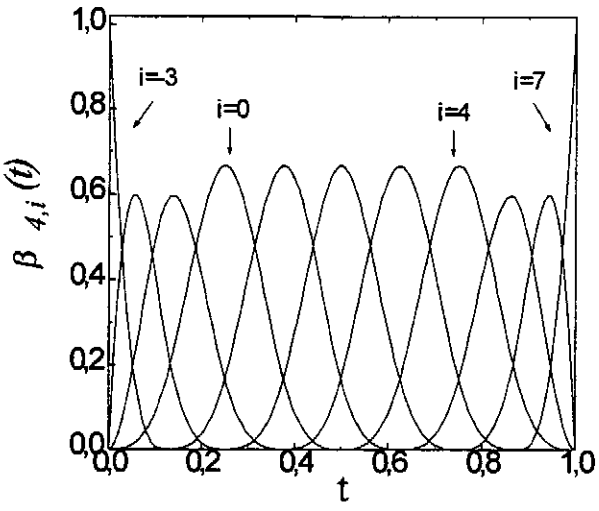

Fig. 2- B-splines basis functions in the unit interval with uniform spacing (K=8).

A third attractive characteristic is that such bases are also local in the sense of a small degree of overlap, i. e. , at every point, except very near the ends of the interval, only three B-splines are non-zero. Moreover, through the use of multiple knots they tend to be more localized and to have a higher spectral content near the ends of the interval. This is just what is needed for an improved description of currents near the edges, where a singular behavior for the currents is expected.

Finally, the analytical simplicity of cubic B-splines is also of importance. In particular, its polynomial form permits a more accurate analytic extraction of singularities when evaluating the integrals that define the elements of the impedance matrix in (7) (see Appendix).

The expression for the basis functions in (6) in terms of the B-splines is written as:

$$f_i^t(t) = t\beta_{4,i-4}(t) \qquad i=1,...,K+n-2=N_t \qquad (10a)$$

$$f_i^{\phi}(t) = \beta_{4,i-4}(t) \qquad i=1,...,K+n-1=N_{\phi} \qquad (10b)$$

The factor t enforces *a priori* the condition $J_t\ (t=0) = 0$ in case of an edge at his point $(\rho(t=0) \neq 0)$ and cancels the factor $1/\rho(t)$ in case of $\rho(t=0) = 0$. It also avoids instabilities in the ϕ current component in regions where J_t dominates both equations in (5) [11], as will be shown in the next section.

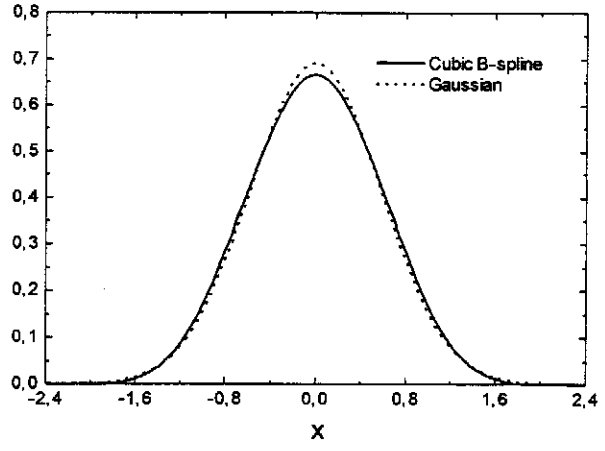

Fig. 3- Cubic B-spline with its corresponding Gabor approximation: $\beta_4(x) \approx (1.5/\pi)^{1/2}\exp(-1.5x^2)$

Two other sets of basis functions are used in the examples of the next section. Entire-domain functions are defined by a series of sinusoids [3]:

$$f_i^t(t) = \sin\left(\frac{i\pi t}{T_f}\right) \qquad i=1,...,N_t \qquad (11a)$$

$$f_i^{\phi}(t) = \cos\left[\frac{(i-1)\pi t}{T_f}\right] \quad i=1,...,N_{\phi} \qquad (11b)$$

Quasi-localized, bandlimited sampling-like functions, are defined as [7], [8]:

$$f_i^t(t) = t\,\mathrm{sinc}\left[\alpha(\kappa t - \tau_i)\right]\mathrm{sinc}(\kappa t - \tau_i) \qquad i=1,...,N_t \qquad (12a)$$

$$f_i^{\phi}(t) = \mathrm{sinc}\left[\alpha(\kappa t - \tau_i)\right]\mathrm{sinc}(\kappa t - \tau_i) \qquad i=1,...,N_{\phi} \qquad (12b)$$

with $\alpha = 0.3$, $\kappa = N_t / T_F$ and $\tau_i = (i-1)$. The above functions are truncated at the first zero of the factor $sinc[\alpha(\kappa t - \tau_i)]$. It gives a negligible degradation on the bandlimited characteristic of these functions, due to the fast decay $(1/d)^2$ they present from the middle-point.

In the examples studied (open bodies), the number of basis functions for t and ϕ components are

related through $N_\phi = N_t + 1$. As a consequence of this choice, the J_t component is forced *a priori* to satisfy the boundary condition at the edge, vanishing at $t = T_F$ (for the case of open bodies) in expansions (10)-(12).

IV. Numerical Results

In this section two numerical examples are presented. The first one involves the determination of the induced current on a 4 λ diameter infinitely thin circular disk. The axially incident electric field is a plane wave x-polarized (Fig. 4). In this case only the $m = \pm 1$ modes will be excited and the current will likewise be x-directed.

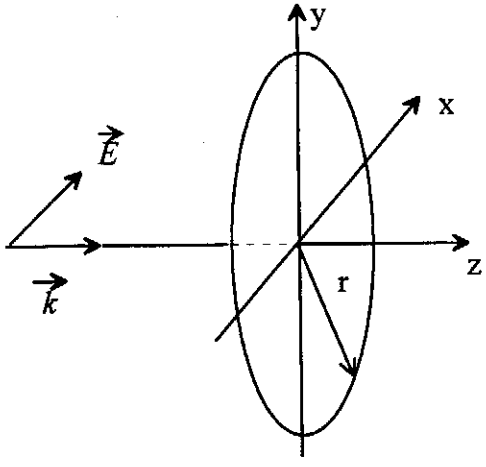

Fig. 4- PEC circular disk illuminated by an axially incident plane-wave

Figs. 5 (a) and (b) show the calculated current (normalized to $|\vec{H}^{inc}|$) when using the three basis sets with $N_t = 10, N_\phi = 11$. The current is t-directed at $\phi = 0^0$ and ϕ-directed at $\phi = 90^0$. For the t-component (Fig. 5(a)), the results obtained are virtually equivalent. The current shows an oscillation with a wavenumber $k \approx k_0$ around the value predicted by the physical optics approximation ($\vec{J}_{PO} = 2\hat{n} \times \vec{H}^{inc}$).

For the ϕ-component (Fig. 5(b)), the currents agree well except for the behavior near the edge. At this point the B-spline expansion produces a better modeling of the current singular behavior. This characteristic is present as the number of basis functions is increased. Fig. 6 illustrates the ϕ-component when employing basis functions with $N_\phi = 19$. The sinusoidal and the sampling-like sets give essentially the same results for the current. A small (apparently non-physical) oscillation in the ϕ-component for the sinusoidal and sampling-like sets can also be observed.

Regarding the CPU time involved in the calculation of the impedance matrix, the sinusoidal (entire-domain) set is clearly the most demanding. The disk is discretized by 20 segments. In each segment, a 5-point Gaussian quadrature is use to integrate over t. Having a spatial support Δ equal to T_F, a total of $100^2=(\Delta/T_F)^2$ integrand evaluations are required to calculate each term of an entire-domain impedance matrix element.

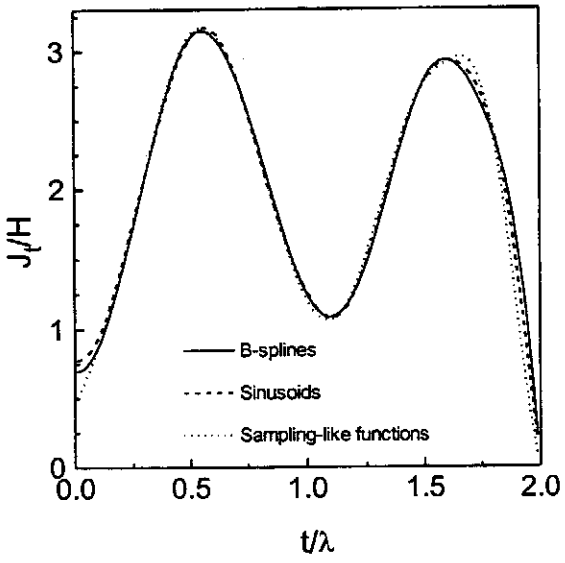

Fig. 5(a)- Induced t- component on a PEC disk. Ten functions used in t direction.

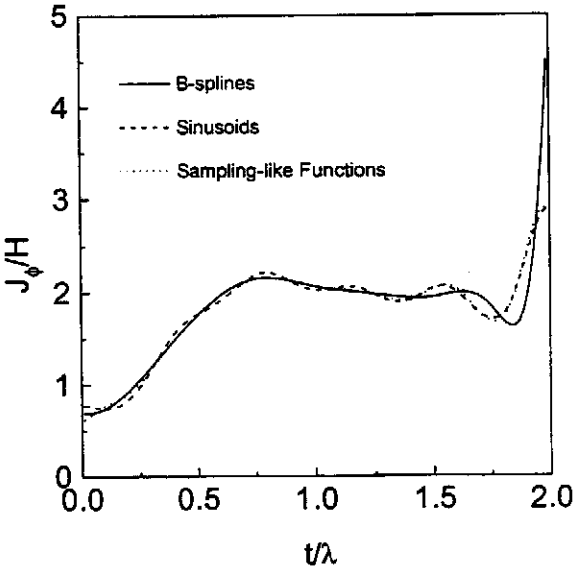

Fig. 5(b)- Induced ϕ- component on a PEC disk. Eleven basis functions used in ϕ direction.

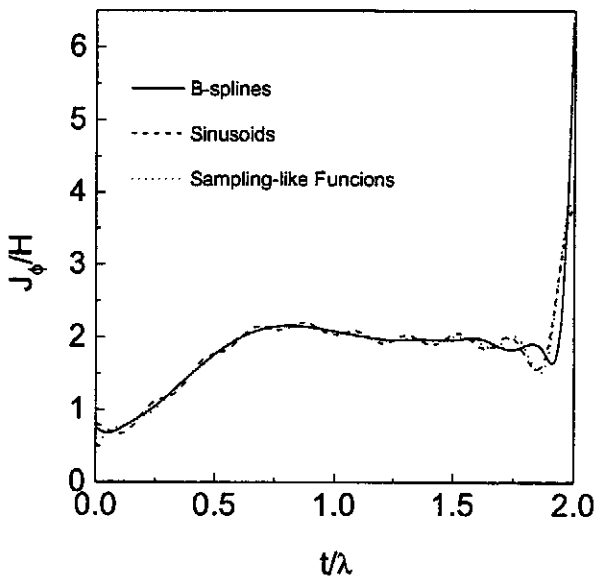

Fig. 6- Induced ϕ- component on a PEC disk. Nineteen basis functions used in ϕ direction.

In the case of sampling-like functions the spatial support (except for the functions near the edge which have a smaller support) equals to $2/\alpha\kappa \approx 6.67T_F/N_t$. When $N_t = 10$, a maximum of approximately $100^2\times(6.67/10)^2$ integrand evaluations for each term in the impedance matrix elements are required, 44% of the entire-domain situation. When $N_t = 18$, this relative number is even smaller, ≈ 13.5%. For the B-spline case, the maximum spatial support equals to $T_F/2$ and $T_F/4$, respectfully. It corresponds to a number of integrand evaluations of 25% ($N_t = 10$) and 6.25% ($N_t = 18$), relative to the entire-domain situation. Table I illustrates those observations, showing the (normalized) overall CPU time required to fill the impedance matrix.

(normalized) CPU TIME		
BASIS FUNCTIONS	*Nt = 10*	*Nt = 18*
Sinusoids	*0.32179*	*1.0000*
Sampling-like	*0.10246*	*0.10728*
B-splines	*0.05475*	*0.05560*

TABLE I

The second numerical example comprises an axially incident plane-wave and a finite hollow cylinder with radius a and extending from $z = 0$ to L (Fig. 7). Twenty segments were used in the discretization of the generating curve. In this example, the strong coupling between the two component equations of EFIE (5) and the dominant behavior of the t-component may cause a spurious oscillatory behavior in the ϕ-component as observed in [11]. This is exactly what happens when B-splines are used without the factor t in the expansion (10a), as Fig. 8(a) depicts.

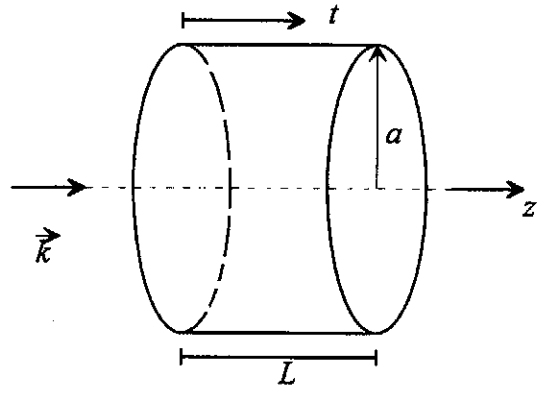

Fig. 7- Finite PEC hollow cylinder illuminated by an axially incident plane wave.

The non-enforcement *a priori* of the boundary condition J_t (t = 0) = 0 for this case also implies a spurious behavior of this component near t = 0 (Fig. 8(b)). In contrast, when the expansion in (11) is used, the spurious result are eliminated, as Figs. 8 (a) and (b) illustrate. Also superposed in these Figures are the currents calculated using sinusoidal functions. In all cases, $N_t = 10$. The same observations previously done with respect to the required CPU time for the matrix fill also apply for this example. Again, the description of the current near the edge with the use of B-splines with multiple knots is more accurate.

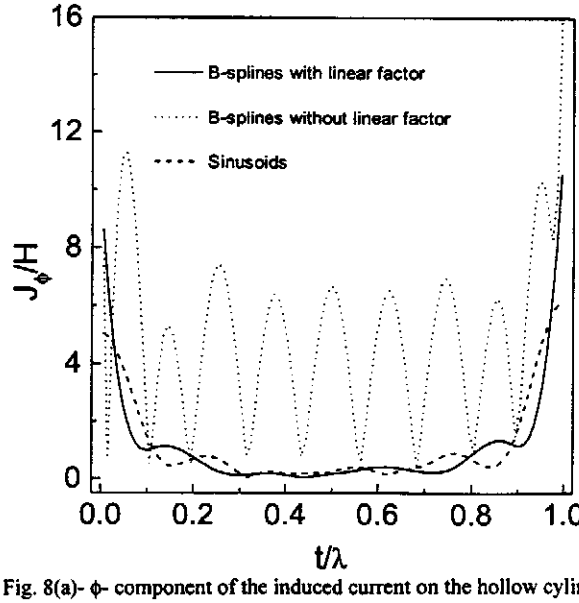

Fig. 8(a)- ϕ- component of the induced current on the hollow cylinder illuminated by an axially incident plane wave.

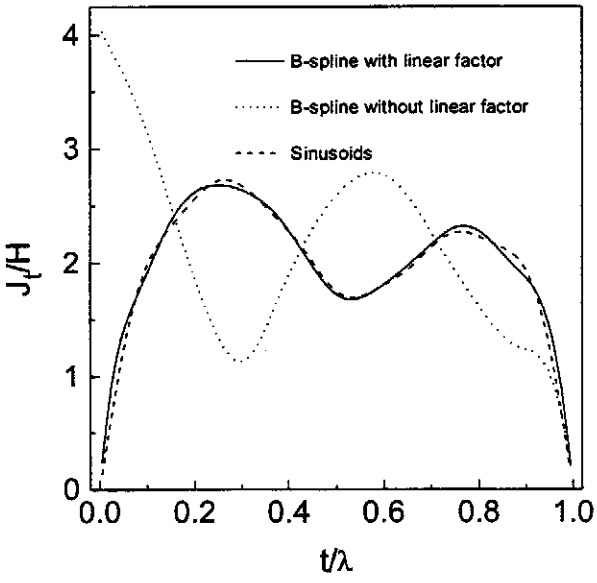

Fig. 8(b)- t- component of the induced current on the hollow cylinder illuminated by an axially incident plane wave.

V. CONCLUSIONS

An adequate choice for the basis functions is of great importance to the computational efficiency of the MoM solution. While a plethora of choices exists, two basic requirements should be satisfied by an efficient basis set: resemblance to the unknown current, thus leading to a convergent solution with few number of terms, and provision of a short computational time.

In this work, different choices for basis functions are addressed in the context of BoR scattering. Concepts like time and frequency localization, as well as the description of the current singularity near the edges, are discussed. It is shown that functions with a limited spectrum can lead to an economic representation in case of smooth BoRs, although near the edge the singular behavior can be overlooked. In this respect, the use of B-splines with multiple knots permitted a more accurate description at the edge. When impedance matrix fill time is compared, entire-domain functions present a basic limitation, as the fill time increases impressively with the number of unknowns. The possibility of eliminating the spurious behavior in the current due to the strong coupling in the EFIE components is investigated. In particular, a linear factor introduced for the t-component, is potentially capable of stabilizing the solution at the same time that it enforces, *a priori*, the boundary conditions.

Two other observations can be made with respect to the implementation of B-splines as basis functions. First, the use of an adaptive mesh grading (AMG) technique arises naturally with B-splines. It consists of concentrating the number of knots in critical regions where a faster variation in the solution is expected. This can be done by redistributing the knot points with respect to, e. g., a weighted combination of the arclength, curvature and edge proximity. Second, B-splines are also present in the context of Multiresolution Analysis (MRA). By using B-splines as a starting point (scaling functions) a sequence of "wavelet subspaces" can be generated [13], with asymptotic convergence to Gabor functions (modulated Gaussian) [10], which are optimally concentrated in both time and frequency domain.

ACKNOWLEDGMENTS

The authors thank Prof. F.J.V. Hasselmann for his useful comments. This research was supported by TELEBRÁS under Contract PUC-TELEBRAS 513/93 - JDPqD.

REFERENCES

[1] R. F. Harrington, "The Method of Moments in Electromagnetics", *J. Electromag. Waves and Appl.*, vol.1, no.3, pp.181-200, 1987.

[2] L. N. Medgyesi-Mitschang and C. Eftimiu, "Scattering from Wires and Open Circular Cylinders of Finite Length Using Entire Domain Galerkin Expansions", *IEEE Trans. Antennas Propag.*, vol.30, no.4, pp.628-636, 1982.

[3] M. R. Barclay and W. V. T. Rusch, "Moment-Method Analysis of Large, Axially Symmetric Reflector Antennas Using Entire-Domain Functions" , *IEEE Trans. Antennas Propag.*, vol.39, no.4, pp.491-496, 1991.

[4] E. Alanen, "Pyramidal and Entire Domain Basis Functions in the Method of Moments", *J. Electromag. Waves and Appl.*, vol.5, no.3, pp.315-329, 1991.

[5] J. R. Mautz and R. F. Harrington, "Radiation and Scattering from Bodies of Revolution" , *Appl. Sci. Res.*, vol.20, pp.405-435, 1969.

[6] A. W. Glisson and D. R. Wilton, "Simple and Efficient Numerical Methods for Problems of Electromagnetic Radiation and Scattering from Surfaces", *IEEE Trans. Antennas Propag.*, vol.28, no.5, pp.593-603, 1980.

[7] G. F. Hermann, "Note on Interpolational Basis Functions in the Method of Moments", *IEEE Trans. Antennas Propag.*, vol.38, no.1, pp.134-137, 1990.

[8] F. L. Teixeira, J. R. Bergmann, "Global vs. Bandlimited Basis Functions in the Analysis of Axisymmetric Reflector Antennas", *IEEE Antennas Propag. Int. Symp. 1995 Digest*, vol.2, pp.1166-1169, 1995.

[9] D. R. Wilton and S. Govind, "Incorporation of Edge Conditions in Moment Method Solutions", *IEEE Trans. Antennas Propag.*, vol.25, no.6, pp.845-850, 1977.

[10] M. Unser, A. Aldroubi and M. Eden, "On the Asymptotic Convergence of B-Spline Wavelets to Gabor Functions" , *IEEE Trans. Information Theory*, vol.38, no.2, pp.864-872, 1992.

[11] W. A.Davis and R. Mittra, "A New Approach to the Thin Scatterer Problem Using the Hybrid Equations", *IEEE Trans. Antennas Propag.*, vol.25, no.3, pp.402-406, 1977

[12] C. de Boor, "On Calculating with B-Splines", *J. Approx. Theory*, vol. 6, pp.50-62, 1972.

[13] C. Goswami, A. K. Chan and C. K. Chui, "On Solving First-Kind Integral Equations Using Wavelets on a Bounded Interval", *IEEE Trans. Antennas Propag.*, vol.43, no.6, pp.614-622, 1995

APPENDIX

The objective of this appendix is twofold. First, it reviews the pseudo-analytic procedure used to remove singularities in the integrals that form the impedance matrix elements. Second, it shows how this singularity extraction can be done in a more exact manner by using B-splines.

The singular integrals that arise in the calculation of impedance matrix elements (7) have the following generic form [5] :

$$I=\int_0^{T_F}dt\int_0^{T_F}dt'\alpha_1(t)\alpha_2(t')\int_0^{\pi}d\phi\cos\phi\cos n\phi\frac{e^{-jkR}}{R}$$

where

$$R=\left[(\rho-\rho')^2+(z-z')^2+4\rho\rho'\sin^2\phi/2\right]^{1/2}$$

and $\alpha_1(t),\alpha_2(t)$ are functions that depend on the choice of basis functions. The above integral has a singularity at $\rho=\rho',z=z',\phi=0$ which does not permit numerical integration. It is rewritten as:

$$I=\int_0^{T_F}dt\int_0^{T_F}dt'\alpha_1(t)\alpha_2(t')\Big[\int_0^{\pi}d\phi(\cos\phi\cos n\phi\frac{e^{-jkR}}{R}-\frac{1}{R})+\int_0^{\pi}\frac{d\phi}{R}\Big]=I_1+I_2$$

I_1 is a proper integral and the singularity is isolated in I_2. Define: $R_1=\left[(\rho-\rho')^2+(z-z')^2\right]^{1/2}$, $\beta_1=\frac{2\sqrt{\rho\rho'}}{R_1}$ and $\xi=\phi/2$; Then:

$$I_2=2\int_0^{T_F}dt\int_0^{T_F}dt'\alpha_1(t)\alpha_2(t')\int_0^{\pi/2}\frac{d\xi}{R_1\sqrt{(1+\beta_1^2\sin^2\xi)}}=2\int_0^{T_F}dt\int_0^{T_F}dt'\alpha_1(t)\alpha_2(t')\frac{K(\beta_2)}{R_2}$$

with $R_2=\left[(\rho+\rho')^2+(z-z')^2\right]^{1/2}$; $\beta_2=\frac{2\sqrt{\rho\rho'}}{R_2}$

where $K(\beta_2)$ is the complete elliptical integral of the first kind. The integral in ϕ was solved, but the above integral is still singular when $\rho=\rho'$ and $z=z'$ (equivalently, $t=t'$). The behavior of $K(\beta_2)$ as $t\to t'$ is given by:

$$\lim_{t\to t'}\frac{K(\beta_2)}{R_2}=\frac{1}{2\rho}\left[\ell n4+\ell nR_2-\ell nR_1\right]$$

Only the last term is singular. It is added and subtracted so that I_2 is written as:

$$I_2=I_{21}-I_{22}=2\int_0^{T_F}dt\int_0^{T_F}dt'\alpha_1(t)\alpha_2(t')\left[\frac{K(\beta_2)}{R_2}+\frac{\ell nR_1}{2\rho}\right]-\int_0^{T_F}dt\int_0^{T_F}dt'\alpha_1(t)\alpha_2(t')\frac{\ell nR_1}{\rho}$$

I_{21} is a proper integral and can be numerically calculated. I_{22} is written as:

$$I_{22}=\frac{1}{2}\int_0^{T_F}dt\frac{\alpha_1(t)}{\rho}\sum_{i=1}^{N}\int_{\varepsilon_i}dt'\alpha_2(t')\ell nR_{1,i}^2$$

where the interval $[0,T_F]$ was divided in N subintervals. Each subinterval defines a segment of the generating curve C where the dependency of ρ' and z' with t' is linearized: $\rho'=\rho_i'+a_i(t'-t_i')$; $z'=z_i'+b_i(t'-t_i')$ and $R_{1,i}^2=(t'-t_{0i})^2+t_{1i}^2$ with $t_{0i}=t_{0i}(t_i',z_i',\rho_i',a_i,b_i)$ and $t_{1i}=t_{1i}(z_i',\rho_i',a_i,b_i)$. In each segment ε_i the function $\alpha_2(t')$ is proportional to the basis function $f_i^p(t')$. The integrals over each ε_i can be evaluate through a local approximation: $\alpha_2(t')\approx a_0+a_1t'+a_2t'^2+a_3t'^3$ since integrals of the form

$$I_{22i}=\int t^n\ell n\left[(t-t_0)^2+t_1^2\right]dt\quad n=0,1,2,3.$$

are tabulated. With the use of B-splines, the coefficients of the local polynomial approximation equal the B-spline coefficients and thus no further numerical error is introduced.